

## OBSTETRICS

# Circular RNAs accumulate in aging human placental tissue and in stillbirth, leading to DNA damage and cellular senescence



Anya L. Arthurs, PhD; Matilda R. Jackson, PhD; Dylan McCullough, BMSc (Hons); Hamish S. Scott, PhD; Christopher P. Barnett, MBBS; Stuart T. Webb, PhD; Melanie D. Smith, PhD; Tanja Jankovic-Karasoulos, PhD; Gustaaf A. Dekker, MD, PhD; Claire T. Roberts, PhD

**BACKGROUND:** Unexplained stillbirth may occur owing to premature placental aging, with an unexpected deterioration of placental function for the gestational age. Circular RNAs are enzyme-resistant RNA molecules that accumulate in aging tissues. Furthermore, circular RNAs bind to genomic DNA directly, forming complexes that can induce DNA breaks and genomic instability.

**OBJECTIVE:** This study investigated tissue aging and circular RNA accumulation with gestational age in healthy and stillbirth placentae and determined whether circular RNAs directly interact with placental DNA, causing DNA damage and cellular senescence.

**STUDY DESIGN:** Placenta samples (n=60 term uncomplicated; n=4 unexplained stillbirth, at 23, 26, 31, and 34 weeks' gestation) were assessed. The abundance of 7 candidate circular RNAs and their linear transcripts was quantified. The physical interaction of candidate circular RNAs with DNA was confirmed. Telomere length, relative abundance of senescence-associated genes, and DNA damage were assessed. Patient-derived trophoblast stem cell differentiation into syncytiotrophoblasts or extravillous trophoblasts was confirmed before circ\_0000284 knockdown. The abundance of circular RNAs in maternal blood sampled between 15 and 16 weeks' gestation (n=12 control, n=6 women who went on to have a stillbirth) was determined using quantitative polymerase chain reaction. Appropriate statistical analyses were undertaken (SPSS).

**RESULTS:** Placental DNA damage, senescence, and expression of 7 candidate circular RNAs, but not their linear transcripts, were increased in 40 and 41+ weeks' gestation samples and in stillbirth compared with earlier gestations (37–39 weeks). DNA:RNA

immunoprecipitation—quantitative polymerase chain reaction signal size confirmed that all candidate circular RNA loci bind to placental DNA. The abundance of circular RNA was significantly decreased with the addition of RNase H1 compared with all healthy gestation samples, indicating that stillbirth placentae may lack RNase H1. Telomere length is shorter in placentae from stillbirths than in healthy 37 weeks' gestation placentae. Depletion of circ\_0000284 by specific small interfering RNA in primary cells significantly reduced DNA damage and increased expression of senescence-associated genes compared with the control. The abundance of candidate circular RNAs is increased in maternal blood at 16 weeks' gestation for women who went on to have a stillbirth compared with women who had live births.

**CONCLUSION:** Stillbirth placentae show accelerated aging with shortened telomeres, premature DNA breaks, increased cellular senescence, and accumulation of candidate circular RNAs at levels consistent with older gestation tissue. These circular RNAs bind to DNA in the placenta, and circ\_0000284 knockdown reduces DNA breaks and senescence in primary placental cells. Therefore, circular RNAs play a role in placental aging and are associated with stillbirth, likely via decreased RNase H1 abundance, preventing circular RNA degradation and facilitating circular RNA accumulation and subsequent circular RNA:DNA complex formation. Circular RNAs may present a viable method of stillbirth risk screening.

**Key words:** aging, circular RNA, DNA, double-stranded breaks, placenta, pregnancy, senescence, stillbirth, telomere

## Introduction

Stillbirth is defined as a fetal death before the birth of a baby of either (1)  $\geq 20$  completed weeks' gestation or (2)  $\geq 400$  g birthweight.<sup>1</sup> Annually, there are 2 million stillbirths worldwide,<sup>2</sup> with  $\sim 2300$  occurring every year in Australia, at a rate unchanged for decades.<sup>1</sup> Although some cases of stillbirth

can be attributed to fetal congenital abnormalities, many cases of stillbirth are “unexplained,” where an autopsy that includes fetal genetics does not establish a cause. Although some risk factors have been identified,<sup>1,3</sup> the etiology of unexplained stillbirth is unknown, and thus, it is impossible to prevent it. One theory for the mechanism underpinning unexplained stillbirth is premature placental aging.

The placenta is a transient organ with a finite life in gestation. Placental aging is a normal phenomenon resulting in physical changes in late gestation without fetal compromise. Accelerated placental aging can occur in stillbirth,

leading to reduced placental functional capacity for fetal support. Although markers of tissue aging, including measures of telomere length<sup>4</sup> and DNA damage,<sup>3–5</sup> are reportedly irregularly high in stillbirth placentae, a direct measure of DNA breaks has not previously been reported.

Tissue aging has been associated with circular RNAs (circRNAs). circRNAs can be generated from most genes and encompass 1 or multiple exonic or intronic regions of RNA. Approximately 20% of all human genes actively transcribe circRNAs.<sup>6</sup> Importantly, they display tissue-specific patterns of expression, making them unique to

0002-9378

© 2025 The Author(s). Published by Elsevier Inc. This is an open access article under the CC BY license (<http://creativecommons.org/licenses/by/4.0/>).  
<https://doi.org/10.1016/j.ajog.2025.08.030>



Click [Supplemental Materials](#) and [Video](#) under article title in Contents at [ajog.org](#)

## AJOG at a Glance

**Why was this study conducted?**

This study was conducted to confirm premature placental aging in cases of unexplained stillbirth and investigate the role of circular RNAs (circRNAs) in the process of placental aging.

**Key findings**

circRNAs accumulate in the aging healthy placenta and accumulate prematurely in stillbirth placentae. circRNAs bind directly to placental DNA, inducing DNA breaks and cellular senescence, thereby contributing to the overall functional decline of the placenta, reducing its ability to support the fetus. circRNAs in maternal blood represent a novel screening tool for the detection of stillbirth risk.

**What does this add to what is known?**

Premature placental aging has previously been associated with stillbirth; however, circRNAs have never before been implicated in this process. circRNA accumulation in aging tissues has been shown in model species (ie, *Caenorhabditis elegans*, *Drosophila melanogaster*, mice) but this is the first evidence in human tissues and in the placenta.

their tissue of origin and the genome of the individual. circRNAs are inherently stable; hence, they can accumulate in tissues with age (previously shown in *Drosophila melanogaster*, *Caenorhabditis elegans*, and murine models<sup>7–9</sup>).

Although circRNAs have many functions,<sup>10</sup> of importance is their ability to directly bind to genomic DNA, forming a circRNA:DNA complex (termed a “circR-loop”).<sup>11</sup> Owing to the steric hindrance, the presence of a circR-loop can cause RNA polymerase II to stall during transcription, subsequently leading to a double-stranded DNA break. This often results in genomic instability,<sup>12</sup> cellular senescence,<sup>13</sup> and cell death.<sup>14</sup> Although their circular form makes them difficult to degrade, RNase H1 can potentially degrade specific circRNAs that form circR-loops, because these maintain a locally open secondary structure<sup>15</sup> (eg, ci-ankrd52<sup>16</sup>).

Given that unexplained stillbirth may be caused by premature placental aging and circRNAs accumulate in aging animal tissues, we sought to determine whether circRNAs accumulate with gestational age in healthy and stillbirth placentae. We further investigated whether select circRNAs bind to DNA to form circR-loops and induce DNA

breaks. We performed in vitro experiments to determine the role of circ\_0000284 in contributing to placental cell senescence and DNA damage. Finally, we investigated the potential use of circRNAs as a screening tool for placental aging culminating in unexplained stillbirth. This study provides novel evidence of circRNA accumulation in aging human tissue and proposes a potential mechanism for stillbirth pathogenesis.

**Methods****Tissue samples**

First-trimester (6–8 weeks' gestation) human placentae were obtained with an informed consent from women undergoing elective termination of pregnancy at the Pregnancy Advisory Centre in the Queen Elizabeth Hospital, in Woodville, South Australia. Ethics approval was obtained from the Central Adelaide Local Health Network Human Research Ethics Committee (HREC/16/TQEH/33, Q20160305). Placentae were collected within minutes of termination, upon which villus tissue was washed with Hanks' balanced salt solution (HBSS; Gibco, Sigma-Aldrich, St. Louis, MO) and transported to the laboratory on ice.

**Healthy placentae from 37 to 41 + weeks' gestation**

Term placentae were obtained at the Lyell McEwin Hospital in Elizabeth, South Australia, from women recruited as part of the Screening Tests to predict poor Outcomes of Pregnancy (STOP) (2015–2018) cohort study.<sup>17</sup> The study was registered with the Australian and New Zealand Clinical Trials Registry (ACTRN 12614000985684). All placentae were associated with uncomplicated pregnancies and were collected from white women. Tissue biopsies from placentae were washed in phosphate-buffered saline (PBS) before being snap frozen and held in liquid nitrogen for 15 minutes, then stored at –80°C. Ethics approval was obtained from the Women's and Children's Health Network Human Research Ethics Committee (HREC/14/WCHN/90; STOP). All women provided a written informed consent.

**Placentae collected from unexplained stillbirths (23, 26, 31, and 34 weeks' gestation)**

Small placental biopsies from unexplained stillbirth cases were obtained from women who had been recruited into the National Health and Medical Research Council— and Genomics Health Futures Mission—Medical Research Future Fund—funded Genomic Autopsy Study.<sup>18</sup> All stillbirths included in the study were classed as unexplained by both clinicians and genomic autopsy. No indication of events during care, clinical management, fetal distress, or congenital or genetic conditions could explain why the stillbirth may have occurred. Placental biopsies were obtained as part of the standard autopsy procedure and were stored at –80°C as approved by the Human Ethics Committee of the Women's and Children's Health Network, South Australia, Australia (HREC/15/WCHN/35), and Melbourne Health as part of the Australian Genomics Health Alliance protocol (HREC/16/MH/251). An informed consent was obtained to allow access to relevant medical information and subsequent storage of anonymized samples, genomic data, and/or medical

information in relevant databases and publications.

### Maternal blood samples collected at 15 to 16 weeks' gestation

Peripheral nonfasting blood samples were collected as part of the STOP cohort study (see earlier) and placed on ice before processing to isolate plasma. Samples were then stored at  $-80^{\circ}\text{C}$  before subsequent analyses.

### Isolation and cultivation of trophoblast stem cells

Trophoblast stem cells (TSCs) were isolated from 5 first-trimester placentae as previously described.<sup>19,20</sup> Briefly, first-trimester villus tissue was washed in HBSS ( $4^{\circ}\text{C}$ ) before manually isolating villus structures for further processing. Villi in HBSS were centrifuged (1000 revolutions per minute [rpm], 1 minute) before 3 consecutive enzymatic digestion steps and density gradient centrifugation as per Haider et al.<sup>21</sup> After careful collection of cells between the 35% and 50% Percoll layers, cells were thoroughly washed with HBSS before being seeded onto fibronectin-coated culture plates ( $20\ \mu\text{g}/\text{mL}$ ; Millipore) using a culture medium to promote stemness (media details in Supplemental Table 1). Cells were cultured for 14 days in humidified incubators at  $37^{\circ}\text{C}$  and 1%  $\text{O}_2$  in 5%  $\text{CO}_2$  (to mimic the in utero first-trimester placental oxygen tension) before differentiating to syncytiotrophoblast or extravillous trophoblast lineages.

### Differentiation of trophoblast stem cells into syncytiotrophoblast and extravillous trophoblast lineages

Patient-derived TSCs were reprogrammed to syncytiotrophoblast or extravillous trophoblast lineages using specific culture media as described in Tan et al.<sup>22</sup> (listed in Supplemental Table 1). TSCs were plated in 6-well plates and cultured in syncytiotrophoblast reprogramming media or extravillous trophoblast reprogramming media for a total of 4 passages. Passaging was completed using TrypLE Express (Gibco) according to the manufacturer's

instructions, and cells were replated at a density of  $\sim 20\%$  (1:5 dilution) per well. At the time of each passage, a portion of the cells were harvested in liquid nitrogen for downstream quantitative polymerase chain reaction (qPCR) analyses. At the end of the passage 4 culture, cells were fixed for visualization or harvested in liquid nitrogen for further experiments.

### Small interfering RNA transfection of trophoblast stem cells

Hallmarks of cellular aging include cellular senescence and DNA damage.<sup>23</sup> circR-loops introduce steric hindrance with the formation of the circRNA:DNA hybrid, which can promote transcriptional pausing and subsequent DNA breaks,<sup>24–26</sup> resulting in genomic instability.<sup>27</sup> As such, we investigated whether circ\_0000284 induces cellular senescence and DNA damage. circ\_0000284 was chosen for investigation because this circRNA had the largest magnitude in fold change expression between 37 and 41+ weeks' gestation placentae (see "Abundance of candidate circular RNAs in the placenta across term and in stillbirth"). This was confirmed using a custom-designed circ\_0000284-specific small interfering RNA (siRNA) in patient-derived TSCs, reprogrammed to syncytiotrophoblasts.

TSCs were reprogrammed to syncytiotrophoblasts as above (see "Differentiation of trophoblast stem cells into syncytiotrophoblast and extravillous trophoblast lineages"). Cultured primary syncytiotrophoblasts were either untreated (control) or treated with a scrambled siRNA or a custom-designed siRNA specific to circ\_0000284. The siRNA sequence was designed to be complementary to the backsplice junction of circ\_0000284 (sequence, ctttattcgagtgattatgattgccatt; scrambled siRNA sequence, tctatcattcatggtatctgtatgat). The siRNA was produced by Thermo Fisher Scientific (Waltham, MA; Silencer Select siRNA). Cells were transfected (in 24-well plates) with the siRNA and scrambled siRNA at 5, 10, and 20 nM final concentrations using Lipofectamine

RNAiMAX (Life Technologies) following the manufacturer's instructions. After optimization, experiments proceeded with a 10 nM final concentration (as the lowest siRNA concentration producing the desired level of knockdown). At 96 hours after siRNA transfection, cells were collected and either (1) immediately used for the Comet assay or (2) snap frozen in liquid nitrogen before storage at  $-80^{\circ}\text{C}$  for subsequent RNA analyses.

### RNA extraction

#### Placenta tissue

Healthy term and stillbirth placental tissues (25 mg) were weighed and washed with PBS. Tissue was disrupted by homogenizing for 3.5 minutes at 30 Hz (TissueLyser, QIAGEN, Hilden, Germany) in 1 mL *TRIzol Reagent* (Sigma-Aldrich). Cultured patient-derived cells were suspended in 1 mL *TRIzol Reagent*. The manufacturer's protocol was then followed to isolate total RNA. The purity and integrity of extracted RNA samples were determined using the Qubit 2.0 fluorometer (Thermo Fisher Scientific). Samples from term and stillbirth placenta tissues were then split into 2 aliquots, with 1 aliquot to be assessed for circRNA expression levels and the other to be assessed for linear transcript expression levels. Samples to be assessed for circRNA expression levels were heated to  $70^{\circ}\text{C}$  for 5 minutes, then immediately cooled below  $40^{\circ}\text{C}$  before incubation with RNase R (10 U/reaction; Astral Scientific, Taren Point, Australia) for 1 hour at  $40^{\circ}\text{C}$ . This step was essential to digest all linear RNAs, leaving only lariat or circRNA structures.

#### Maternal blood

Total RNA was isolated from  $200\ \mu\text{L}$  thawed frozen plasma using the miR-Neasy serum/plasma kit (QIAGEN), according to the manufacturer's instructions and as per Vilades et al.<sup>28</sup>

### RNA quantification

Total RNA for each sample from term and stillbirth placenta tissues, after

incubation of 1  $\mu$ g of RNA either with RNase R or untreated, was quantified using the Qubit 2.0 fluorimeter (Thermo Fisher Scientific). Total RNA from maternal blood samples was quantified using the Qubit 2.0 fluorimeter as is. As per Drula et al,<sup>29</sup> Qubit measurement was accomplished with the Qubit RNA High Sensitivity assay kit using 1  $\mu$ L of the RNA sample, 198  $\mu$ L of the Qubit kit working solution, and 1  $\mu$ L of the provided fluorophore, as per the manufacturer's instructions. One proposed method for endogenous circRNA degradation is via RNase H1,<sup>16</sup> specifically for circRNAs that can form circR-loops with template DNA owing to their locally open secondary structure. RNase H1 cleaves the circR-loop and, in some cases, further degrades the circRNA. RNA amount as determined by Qubit was normalized based on the standard curve and input and compared between RNase R-treated and untreated groups, in the presence and absence of RNase H1-specific siRNA (as per Wu et al<sup>30</sup>) per sample to quantify bulk circRNA abundance.

### Complementary DNA synthesis and quantitative polymerase chain reaction

Synthesis of complementary DNA was conducted beginning with 1  $\mu$ g of total RNA using the QuantiNova reverse transcription kit (QIAGEN) according to the manufacturer's protocol. qPCR was performed in triplicate and conducted with SYBR Green (QIAGEN) according to the manufacturer's instructions, with *YWHAZ*, *GAPDH*, and *ACTB* as housekeeping genes (all primer sequences in Supplemental Table 2). Custom divergent primers were designed for each circRNA, flanking the backsplice junction, with an amplicon size of <300 base pairs. As an additional confirmation of amplification specificity, all primers were assessed using the primer design BLAST tool.<sup>29</sup> Furthermore, primer specificity was confirmed via melt curve analysis from reverse transcription qPCR. The qPCR conditions were PCR initial activation at 95°C

for 5 minutes, followed by 50 cycles of 95°C for 15 seconds, melt temperature (detailed in Supplemental Table 2) for 40 seconds, and 72°C for 20 seconds. qPCR results were analyzed using the  $2^{-\Delta\Delta CT}$  method.<sup>31</sup> Samples were sorted into groups depending on the gestational age of tissue (see Table for numbers and characteristics of women's samples used).

Candidate circRNAs were chosen from pilot sequencing studies. Differentially expressed circRNAs between gestational time points of 37 and 41+ weeks were selected for further study.

### Telomere length analysis

Genomic DNA was extracted from samples using the DNeasy Blood and Tissue Kit (QIAGEN), starting with 25 mg tissue. Telomere length was assessed according to the optimized protocol outlined by Cawthon (2009).<sup>32</sup> Standard curves were generated for telomere lengths from single-copy gene amplifications using a reference DNA. The telomere length for each sample was derived based on the ratio of telomere length between the sample and the single-copy gene standard (*T/S* ratio).

### Comet assay

The Abcam Comet assay kit (ab238544; Abcam) was used to assess DNA damage in isolated trophoblasts, as per the manufacturer's instructions. For each sample from term and stillbirth placenta tissues, approximately 25 mg tissue (stored at -80°C) was used. For each sample from cultured early gestation patient samples,  $2.5 \times 10^5$  cells were used. Alkaline electrophoresis was performed. The DNA integrity of 100 cells per placenta was analyzed using CometScore 2.0 software (RexHoover.com). The fluorescence intensity of the Comet "tail" was used as a measure of DNA damage (indicated as tail DNA %). Tail DNA was shown as a percentage increase in damage relative to averaged control samples. Representative images of healthy cells (Figure 2, C) and DNA-damaged cells (Figure 2, D) are included for reference.

### DNA:RNA immunoprecipitation

DNA:RNA immunoprecipitation (DRIP)-qPCR was used to detect circR-loops (DNA:RNA complexes; Figure 1, I) in pooled placenta samples from gestations 37 to 41+ weeks, to determine whether circRNAs that accumulate in the aging placenta interact directly with DNA. DRIP was performed according to steps 3 to 25 in the protocol published by Sanz and Chédin (2019),<sup>33</sup> with some notable exceptions for where tissue was used as a starting material instead of cultured cells. Tissue was first prepared as follows before progressing to step 3 of the protocol.

Approximately 50 mg frozen placental villous tissue was submerged in 1 mL RLT+ buffer (QIAGEN) with added 0.01% (v/v)  $\beta$ -mercaptoethanol and 0.5% (v/v) Reagent DX (QIAGEN) with 1 g beads. The tissue was disrupted by homogenizing for 3.5 minutes at 30 Hz (TissueLyser, QIAGEN). Cell suspensions were centrifuged (3 minutes, maximum speed, 4°C) before removal of the supernatant. The cell pellet was washed (sterile Dulbecco's PBS, 5 mL) before centrifugation (3 minutes, 1000 rpm, 4°C) and removal of the supernatant. Steps 3 to 25 of the protocol<sup>33</sup> were then followed.

After completing DRIP, DRIP-qPCR analysis was undertaken using either predesigned primers<sup>33</sup> for known R-loop-positive loci *TFPT* and *CALM3* and known R-loop-negative locus *EGFR1neg* or custom-designed primers (Supplemental Table 2) to target the backsplice junctions of circ\_0009000, circ\_0024157, circ\_0061017, circ\_0036877, circ\_0054624, circ\_0111277, and circ\_0000284. All DRIP-qPCR analyses were completed both in samples treated with and without RNase H treatment before DRIP. Because RNase H cleaves the RNA of RNA:DNA hybrids, it is expected that the addition of RNase H to the sample will result in a significantly suppressed R-loop signal and hence a reduced DRIP-qPCR signal (functioning as a negative control). This was confirmed in our results.

TABLE

## Characteristics of women and infants from the study by gestational age group (weeks)

Characteristic	Gestational age group (wk)					Stillbirth
	37	38	39	40	41+ <sup>a</sup>	
Maternal age (y)	28.7±1.5	24.1±2.9	25.9±1.9	28.3±4.5	26.8±4.2	#1: 35 #2: 26 #3: 33 #4: 28
Maternal BMI (kg/m <sup>2</sup> )	26.4±5.8	27.2±9.1	23.1±4.3	20.8±4.1	23.4±6.2	#1: DM #2: DM #3: DM #4: 22.8
Smoking status <sup>b</sup>	1/12	2/12	1/12	3/12	2/12	#1: DM #2: DM #3: DM #4: N
Gestational age (wk)	37.1±0.9	38.0±0.3	39.1±0.7	40.0±0.4	41.5±0.3	#1: 23 #2: 26 #3: 34 #4: 31
Birthweight (g)	2962±325	3345±465	3089±201	3702±161	3513±277	#1: 256 #2: 800 #3: 2546 #4: 1140
Fetal sex <sup>c</sup>	XX=6 XY=6	XX=6 XY=6	XX=7 XY=5	XX=6 XY=6	XX=6 XY=6	#1: XX #2: XY #3: XY #4: XX

Data are presented as mean±standard error of the mean.

BMI, body mass index; DM, data missing, given that data were not available at the time of sample collection.

<sup>a</sup> The group "41+ weeks' gestation" is defined as delivery at 41+0 through to 41+6 weeks' gestation; <sup>b</sup> Smoking status as self-reported by the patient at the time of delivery. X/12 indicates the number of women who reported yes to smoking while pregnant of the total 12 women. For stillbirths, Y, yes; N, no; <sup>c</sup> Where XX is female and XY is male.

Arthurs. Circular RNAs, placental aging, and stillbirth. *Am J Obstet Gynecol* 2026.

## Immunocytochemistry of cultured trophoblast stem cells

Immunocytochemistry was performed as described by Morosin et al<sup>34</sup> (2020). Briefly, fixed cells were permeabilized in 0.1% Triton X-100 in PBS (Bio-Rad) before being blocked in 1% bovine serum albumin. Cells were either incubated with an E-cadherin primary antibody (Abcam ab1416; syncytiotrophoblast lineage only) or a human leukocyte antigen G (HLA-G) primary antibody (Invitrogen MA1-10359; extravillous trophoblast lineage only) before being washed with PBS and incubated with Alexa Fluor 488 goat anti-mouse IgG (H+L) secondary antibody (Thermo Fisher Scientific, A-11001). Negative controls were included where cells were incubated in the

absence of either the primary antibody or both the primary and secondary antibodies. Cells were mounted onto microscope slides using a DAPI mounting medium (ProLong Diamond Antifade Mountant with DAPI; Invitrogen). Slides were stored at 4°C, and 3 images were taken per slide (imaged areas were selected at random) using confocal microscopy at 40× magnification.

Syncytialization was observed where multiple nuclei (blue) existed within 1 E-cadherin boundary (green). Cells were classed as extravillous trophoblasts where HLA-G was expressed.

## Statistical analysis

Statistical analysis for differences between groups for qPCR and Comet assay data was undertaken using SPSS

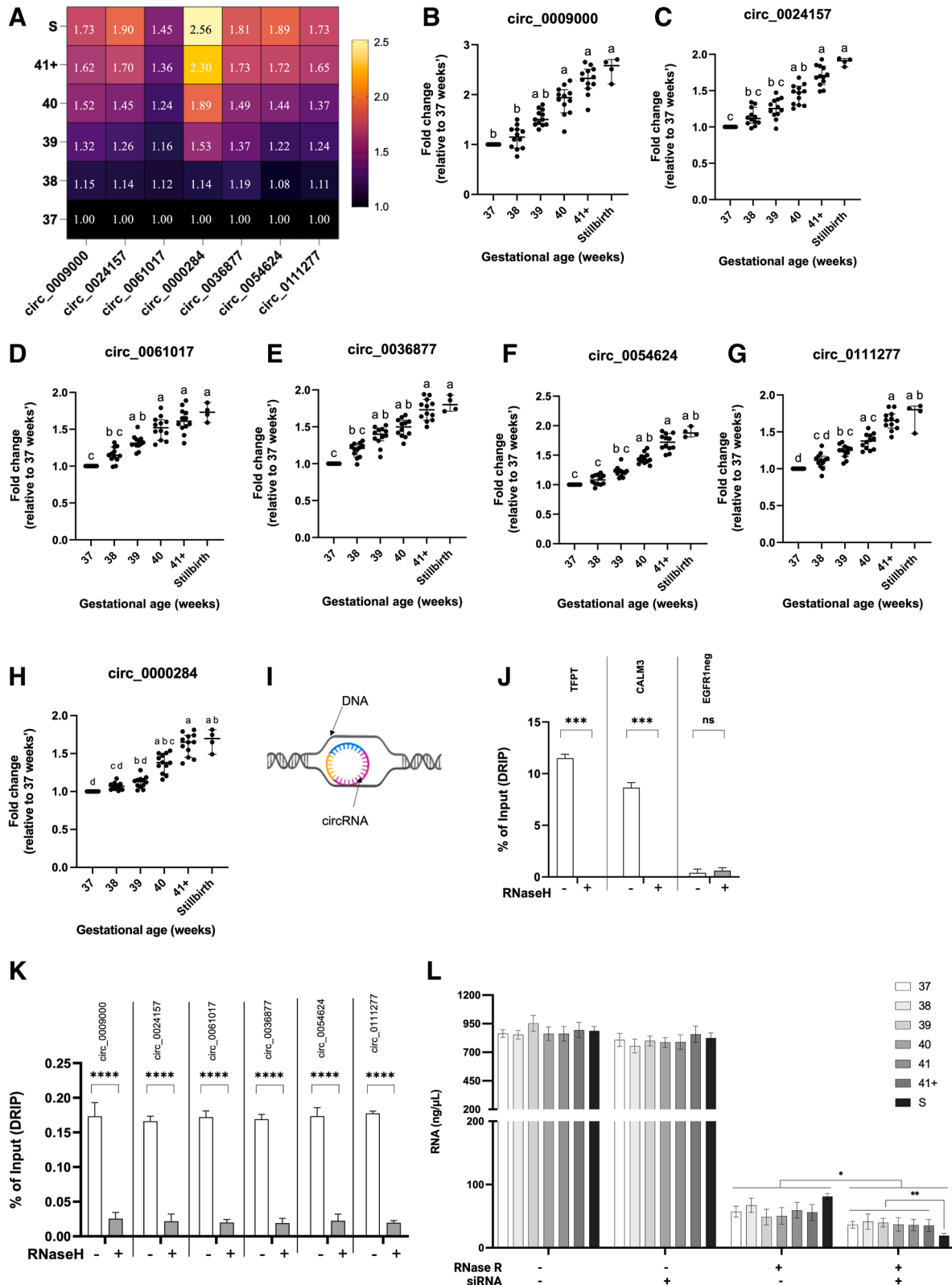
statistics software. Outliers were removed from the data using a Grubbs' test. Data were assessed for normality distribution, and either a Kruskal-Wallis or 2-way ANOVA test was conducted. Adjustments were made for multiple comparisons (Tukey's). Differences between groups were considered significant at  $P<.05$ .

## Results

### Cohort characteristics

Placenta samples were available from 60 women who had healthy pregnancies (n=12 per gestational group) and 4 women who experienced stillbirth. All stillbirths had been assessed by clinical pathologists as "unexplained foetal deaths," with no noted congenital anomalies.

**FIGURE 1**  
Abundance of circRNAs in placenta, and interaction with DNA



**A**, Heat map depicting abundance values (as fold change relative to abundance at 37 weeks' gestation) of **(B)** circ\_0009000, **(C)** circ\_0024157, **(D)** circ\_0061017, **(E)** circ\_0036877, **(F)** circ\_0054624, **(G)** circ\_0111277, and **(H)** circ\_0000284, in isolated cells from 37, 38, 39, 40, and 41+

Maternal and birth characteristics are presented in Table.

### Abundance of candidate circular RNAs in the placenta across term and in stillbirth

All relative abundance values, expressed as fold change compared with the abundance in placenta at 37 weeks' gestation, are listed in Figure 1, A. *P* values for multiple comparisons are presented in Supplemental Table 3. The relative abundance of circ\_0009000 (Figure 1, B) was significantly increased in placenta from 40 and 41+ weeks' gestation, as well as in placenta from stillbirths. The relative abundance of circ\_0024157 (Figure 1, C) was significantly increased in placenta from 40 and 41+ weeks' gestation, as well as in placenta from stillbirths. The relative abundance of circ\_0061017 (Figure 1, D) was significantly increased in placenta from 39, 40, and 41+ weeks' gestation, as well as in placenta from stillbirths. The relative abundance of circ\_0036877 (Figure 1, E) was significantly increased in placenta from 39, 40, and 41+ weeks' gestation, as well as in placenta from stillbirths. The relative abundance of circ\_0054624 (Figure 1, F) was significantly increased in placenta from 40 and 41+ weeks' gestation, as well as in placenta from stillbirths. The relative abundance of circ\_0111277 (Figure 1, G) was significantly increased in placenta from 39, 40, and 41+ weeks' gestation, as well as in placenta from stillbirths. The relative abundance of circ\_0000284 (Figure 1, H) was significantly increased in placenta from 40 and 41+ weeks' gestation, as well as in placenta from stillbirths.

### Candidate circular RNAs bind to DNA to create circular RNA:DNA complexes in term placenta

According to Sanz and Chédin,<sup>33</sup> R-loop positive loci are typically recovered with an efficiency ranging from 1% to 15% of the total input, whereas negative loci are typically recovered with values of <0.1%. This was replicated in our results for placenta tissue (Figure 1, J), where *TFPT* (mean, 11.499%; *P*=.0008) and *CALM3* (mean, 8.644%; *P*=.0009) produced DRIP-qPCR signals, shown as a % of the total DRIP input, significantly larger than those of their RNase H-treated controls. There was no significant difference between the DRIP-qPCR signals of *EGFR1-neg* (mean, 0.389%) with and without RNase H treatment.

DRIP-qPCR signal for circ\_0009000 (mean, 0.173%; Figure 1, K), circ\_0024157 (mean, 0.166%), circ\_0061017 (mean, 0.172%), circ\_0036877 (mean, 0.169%), circ\_0054624 (mean, 0.173%), circ\_0024157 (mean, 0.177%), and circ\_0000284 (mean, 0.163%) was significantly larger than their RNase H-treated controls (all *P*<.0001).

### Circular RNAs, which accumulate in the aging placenta and in the stillbirth placenta, are subject to RNase H1 degradation

We assessed whether circRNAs in placenta samples from uncomplicated and stillbirth placenta were subject to RNase H1 degradation. The quantity of total RNA for each sample was unchanged with the administration of an siRNA that specifically targets RNase H1 (Figure 1, L). For samples taken from uncomplicated pregnancies

delivering at 37, 38, 39, 40, and 41+ weeks' gestation and in stillbirth placenta, the quantity of circRNA (after total RNA treatment with RNase R) was significantly decreased with the administration of the RNase H1-specific siRNA (*P*<.05). Furthermore, the quantity of circRNAs was significantly lower after the administration of RNase H1-specific siRNA in placenta from stillbirths than all other gestations (*P*<sub>37</sub>=.0094; *P*<sub>38</sub>=.0087; *P*<sub>39</sub>=.0072; *P*<sub>40</sub>=.0090; *P*<sub>41+</sub>=.0099), indicating that circRNAs from unexplained stillbirth placenta are more susceptible to RNase H1 degradation, likely indicating a deficiency of endogenous RNase H1 in these samples.

### Telomere length is decreased in stillbirth compared with healthy term placenta tissue

Relative telomere lengths (Figure 2, A) were significantly reduced by ~40% in stillbirth (3.108±1.954) compared with healthy placenta from 37 weeks' gestation (5.881±2.823; *P*<.05). There were no other significant differences in relative telomere lengths among 37, 38 (5.321±2.390), 39 (5.119±2.943), 40 (4.794±2.510), and 41+ weeks' gestation (4.564±2.428) and stillbirth.

### Expression of senescence-associated genes is increased in aged healthy and stillbirth placenta tissue

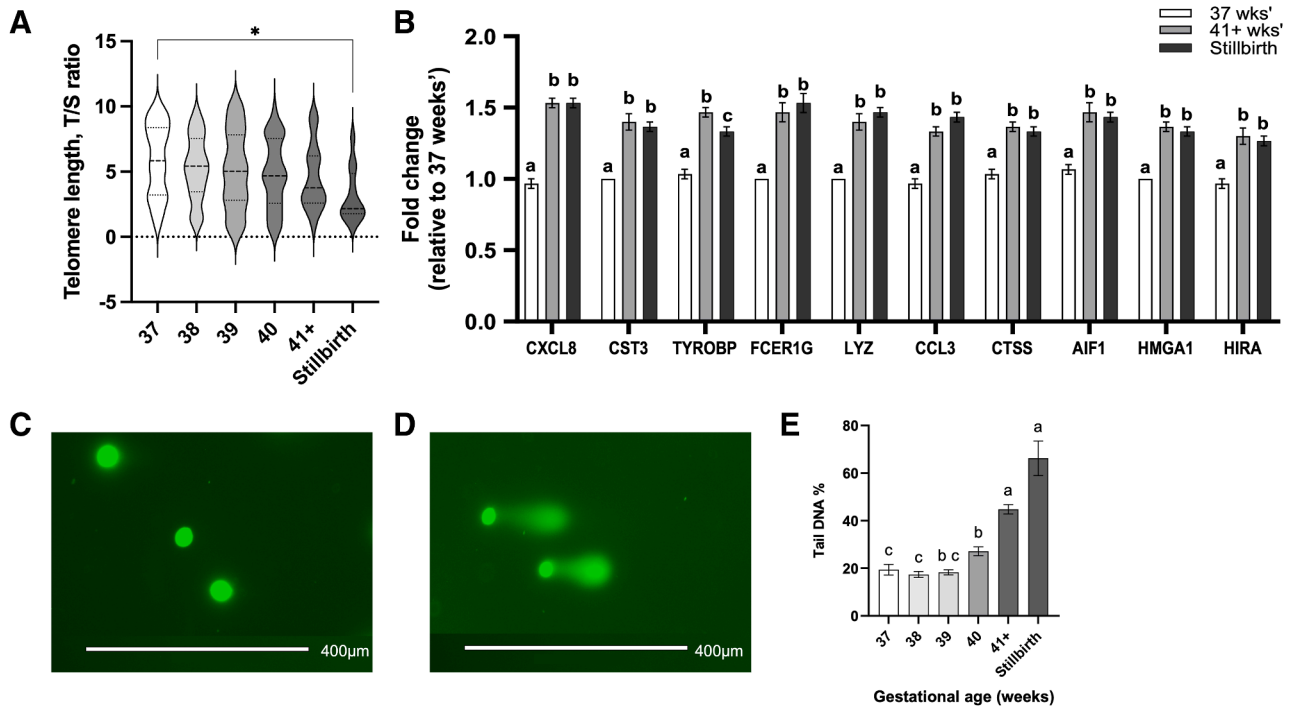
Saul et al<sup>35</sup> validated a gene set that identifies senescent cells and predicts senescence-associated pathways in tissue. Messenger RNA (mRNA) expression of senescence-associated genes (Figure 2, B) was significantly increased

uncomplicated and stillbirth placenta. n=12 placenta/uncomplicated gestational group, n=4 stillbirth placenta. Data are presented as scatter plots with bars and indicate mean±standard error of the mean. I, Diagram of circR-loop, where the circRNA molecule binds to 1 strand of helically unwound DNA. DRIP-qPCR analysis using primers for (J) R-loop-positive loci *TFPT* and *CALM3* and R-loop-negative locus *EGFR1neg* and (K) circ\_0009000, circ\_0024157, circ\_0061017, circ\_0036877, circ\_0054624, circ\_0111277, and circ\_0000284. Where indicated, samples were treated with RNase H before DRIP. Treatment with RNase H significantly suppressed the DRIP-qPCR signal, consistent with R-loop formation in the tested regions. n=5 placenta with, and n=5 placenta without, RNase H treatment. DRIP-qPCR signal intensity shown as % of input (DRIP), with indication of mean±standard error of the mean. L, Quantity of total RNA (ng/μL), starting with ~1 μg total in isolated cells from 37, 38, 39, 40, and 41+ uncomplicated and stillbirth placenta. n=12 placenta/uncomplicated gestational group, n=4 stillbirth placenta. RNA quantified in the presence and absence of RNase R (degrades linear transcripts) and an siRNA specific for RNase H1 (enzyme that can degrade circRNAs). Different letters represent statistically significant (*P*<.05) differences. \*\*\**P*<.001 and \*\*\*\**P*<.0001.

circR-loop, circRNA:DNA complex; circRNA, circular RNA; DRIP, DNA:RNA immunoprecipitation; ns, not significant; qPCR, quantitative polymerase chain reaction; siRNA, small interfering RNA.

Arthurs. Circular RNAs, placental aging, and stillbirth. *Am J Obstet Gynecol* 2026.

**FIGURE 2**  
Tissue aging across physiologic term and in unexplained stillbirth



**A**, Telomere length (expressed as “T/S ratio,” ie, quantity of telomere DNA divided by the quantity of a single-copy gene). **B**, Fold change mRNA expression of senescence-associated genes in placenta tissue from 37 weeks’ gestation uncomplicated pregnancy (white), 41+ weeks’ gestation uncomplicated pregnancy (gray), and stillbirth (black). Data are presented as **(A)** violin plots and **(B)** mean±standard error of the mean. Representative images of **(C)** healthy cells and **(D)** DNA-damaged cells, as imaged using epifluorescent microscopy after performing a Comet assay. **E**, Levels of DNA damage, as assessed by tail DNA %, in isolated cells from 37, 38, 39, 40, and 41+ uncomplicated and stillbirth placentae. n=12 placentae/uncomplicated gestational group, n=4 stillbirth placentae; 100 cells analyzed after the Comet assay, per placenta. Data are presented as mean±standard error of the mean. Different letters represent statistically significant ( $P<.05$ ) differences. \* $P<.05$ .

mRNA, messenger RNA.

Arthurs. Circular RNAs, placental aging, and stillbirth. *Am J Obstet Gynecol* 2026.

in 41+ weeks’ gestation healthy placentae (all  $P<.0001$ ) and stillbirth placentae ( $P_{CXCL8}<.0001$ ;  $P_{CST3}<.0001$ ;  $P_{TYROBP}=.0003$ ;  $P_{FCER1G}<.0001$ ;  $P_{LYZ}<.0001$ ;  $P_{CCL3}<.0001$ ;  $P_{CTSS}<.0001$ ;  $P_{AIF1}<.0001$ ;  $P_{HMGA1}<.0001$ ;  $P_{HIRA}<.0001$ ) compared with 37 weeks’ gestation healthy placentae.

mRNA expression of *TYROBP* only was significantly increased in 41+ weeks’ gestation healthy placentae compared with stillbirth placentae ( $P=.0038$ ).

### DNA damage is increased in aged healthy and stillbirth placenta tissue

Tail DNA % was significantly higher in cells from placentae sampled at 40 weeks’ gestation than 37 and 38 weeks’ gestation

( $P_{37}=.0381$ ;  $P_{38}=.0203$ ; Figure 2, E) and 41+ weeks’ gestation than 37, 38, 39, and 40 weeks’ gestation (all  $P<.0001$ ) and in placentae from stillbirths than 37, 38, 39, and 40 weeks’ gestation ( $P_{37}<.0001$ ;  $P_{38}<.0001$ ;  $P_{39}<.0001$ ;  $P_{40}=.0001$ ).

### circ\_0000284 is primarily expressed in syncytiotrophoblasts

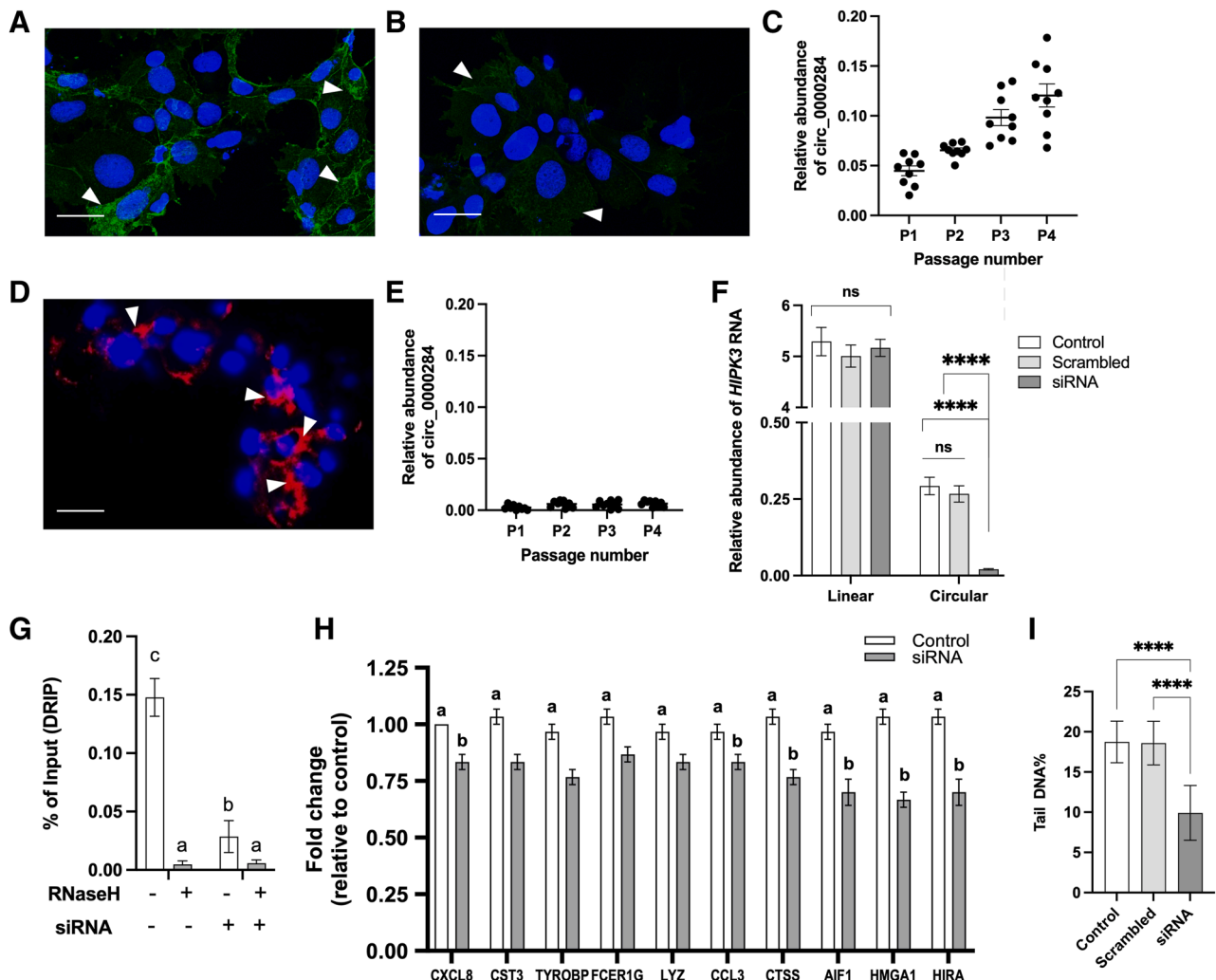
Patient-derived TSCs (Figure 3, A) were isolated and underwent cellular reprogramming to either syncytiotrophoblasts (Figure 3, B) or extravillous trophoblasts (Figure 3, D). qPCR detected circ\_0000284 in syncytiotrophoblasts (Figure 3, C), where its abundance increased with each passage (mean,  $P_1=0.045$ ,  $P_2=0.064$ ,  $P_3=0.098$ ,  $P_4=0.120$ ), but was not detected in extravillous trophoblasts (Figure 3, E).

### In vitro knockdown of circ\_0000284 Validation of the small interfering RNA knockdown

As shown in Figure 3, F, transfection with the scrambled siRNA did not alter the expression of the linear *HIPK3* mRNA (shown as abundance relative to *YWHAZ* and *ACTB*) compared with the control. Importantly, administration of the siRNA specific to circ\_0000284 did not alter the expression of linear *HIPK3* mRNA. However, the siRNA successfully reduced the relative abundance of circ\_0000284 compared with both the untreated cells (control) and cells treated with the scrambled siRNA (all  $P<.0001$ ).

DRIP-qPCR confirmed that circ\_0000284 forms a circR-loop in primary syncytiotrophoblasts (mean, 0.148%;  $P<.0001$ , compared with RNase

**FIGURE 3**  
In vitro confirmation of circRNA mechanism of action



Representative immunocytochemistry images of (A) not syncytialized TSCs, (B) syncytialized TSCs (ie, reprogrammed to syncytiotrophoblasts), and (D) TSCs reprogrammed to extravillous trophoblasts. Scale bars: 10  $\mu$ m. Nuclei are stained with DAPI (blue), green stain is for E-cadherin (cell membrane), and red stain is for HLA-G (expressed in extravillous trophoblasts). White arrows indicate E-cadherin staining (A, B) and HLA-G staining (D). Relative abundance of circ\_0000284 in cultured (C) syncytiotrophoblasts and (E) extravillous trophoblasts, over 4 culture passages. Data are presented as scatter plots with bars and indicate mean  $\pm$  standard error of the mean. F, Abundance of HIPK3 RNA ("linear") and circ\_0000284 ("circular") in cultured syncytiotrophoblast cells, either untransfected ("control") or transfected with a scrambled siRNA ("scrambled") or an siRNA specific to circ\_0000284 ("siRNA"). G, DRIP-qPCR using primers for circ\_0000284, in syncytiotrophoblasts treated with combinations of RNase H and siRNA as indicated. H, Fold change mRNA expression of senescence-associated genes in syncytiotrophoblasts, either untreated (white) or treated with siRNA (gray). I, Levels of DNA damage, as assessed by tail DNA %, in syncytiotrophoblast cells. n=5 patients/group; 100 cells analyzed after the Comet assay, per sample. Data are presented as mean  $\pm$  standard error of the mean. Different letters represent statistically significant ( $P < .05$ ) differences. \*\*\*\* $P < .0001$ .

DRIP, DNA:RNA immunoprecipitation; HLA-G, human leukocyte antigen G; mRNA, messenger RNA; ns, not significant; qPCR, quantitative polymerase chain reaction; siRNA, small interfering RNA; TSC, trophoblast stem cell.

Arthurs. Circular RNAs, placental aging, and stillbirth. Am J Obstet Gynecol 2026.

H-treated control; Figure 3, G) and administration of the siRNA specific to circ\_0000284 significantly reduced circR-loop formation (mean, 0.029%;  $P < .0001$ ).

### Expression of senescence-associated genes is attenuated with depletion of circ\_0000284

mRNA expression of senescence-associated genes (Figure 3, H) was

significantly decreased in cells transfected with the siRNA specific to circ\_0000284 compared with the control; CXCL8 ( $P = .0053$ ), CCL3 ( $P = .0291$ ), CTSS ( $P < .0001$ ), AIF1

( $P < .0001$ ), *HMGA1* ( $P < .0001$ ), and *HIRA* ( $P = .0005$ ). mRNA expression of *CST3*, *TYROBP*, *FCER1G*, and *LYZ* was not significantly changed.

### DNA damage is mitigated with depletion of circ\_0000284

Transfection with the siRNA specific to circ\_0000284 in primary syncytiotrophoblasts significantly reduced the level of DNA damage (tail DNA %; Figure 3, I) compared with both the control (reduced by 41.3%) and scrambled groups (reduced by 39.5%) (all  $P < .0001$ ). Transfection with the scrambled siRNA did not alter the level of DNA damage (tail DNA %)

compared with the control, indicating that depletion of circ\_0000284 results in reduced DNA damage.

### Circular RNAs can be detected in blood as a proxy measurement of placental aging

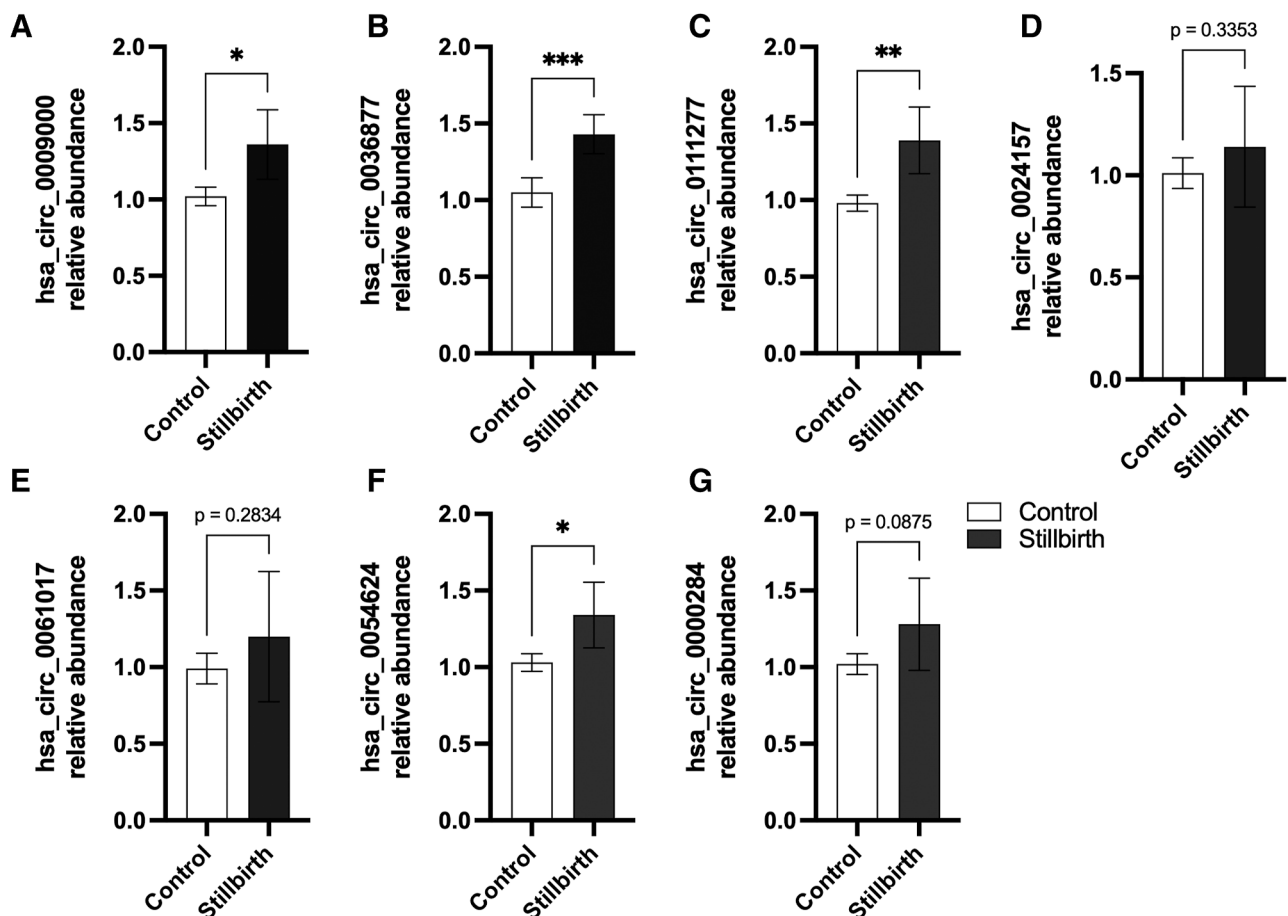
Candidate circRNAs hsa\_circ\_0009000 ( $P = .0137$ ), hsa\_circ\_0036877 ( $P = .0002$ ), hsa\_circ\_011277 ( $P = .0052$ ), and hsa\_circ\_0054624 ( $P = .0158$ ) were significantly more abundant (Figure 4) in maternal blood sampled at 15 to 16 weeks' gestation in women who went on to have a stillbirth than in women who delivered live babies. The abundance of hsa\_circ\_0024157, hsa\_circ\_0061017,

and hsa\_circ\_0000284 was not significantly changed between groups.

### Comment Principal findings

Here, we confirm that placentae from stillbirths experience accelerated aging (as determined by typical hallmarks of decreased telomere length, increased rates of cellular senescence, and DNA damage). circRNAs circ\_0009000, circ\_0024157, circ\_0061017, circ\_0036877, circ\_0054624, circ\_011277, and circ\_0000284 accumulate in aging placental tissue and prematurely accumulate in stillbirth placentae. These circRNAs bind to placenta DNA,

**FIGURE 4**  
Abundance of circRNAs in maternal blood at 15-16 weeks' gestation



Abundance (as fold change relative to housekeeping genes) of (A) hsa\_circ\_0009000, (B) hsa\_circ\_0036877, (C) hsa\_circ\_011277, (D) hsa\_circ\_0024157, (E) hsa\_circ\_0061017, (F) hsa\_circ\_0054624, and (G) hsa\_circ\_0000284 in maternal blood sampled at 15 to 16 weeks' gestation from women who went on to have a stillbirth and women who had live births.  $n = 12$ /live births,  $n = 6$ /stillbirth group. Data are presented as mean  $\pm$  standard deviation. \* $P < .05$ , \*\* $P < .01$ , and \*\*\* $P < .001$ . Results are considered statistically significant if  $P < .05$ .

Arthurs. Circular RNAs, placental aging, and stillbirth. *Am J Obstet Gynecol* 2026.

facilitating DNA breaks and cellular senescence. Measurement of candidate circRNAs in maternal blood sampled at 15 to 16 weeks' gestation is a potential screening tool to indicate premature placental aging indicative of stillbirth risk, although this requires large-scale validation at a population level.

## Results in the context of what is known

### The accumulation of circular RNAs

The accumulation of circRNAs in aged tissue is a relatively recent discovery, evident from studies<sup>36</sup> using *Drosophila melanogaster* photoreceptor neurons,<sup>37</sup> mouse brain and heart,<sup>9</sup> and *Caenorhabditis elegans*.<sup>8</sup> It is likely that circRNAs accumulate in tissues because their lack of a 5' cap and a polyadenylated tail renders them resistant to exoribonuclease degradation.<sup>38</sup> Another explanation for circRNA accumulation in some tissues is that, in cell types such as neurons, rates of mitosis and proliferation are lower than those of other cell types, allowing for reduced turnover of circRNAs.<sup>36,39–41</sup> Given that the nuclei of the syncytiotrophoblast are non-mitotic,<sup>42</sup> transcription is significantly reduced,<sup>43</sup> and the syncytiotrophoblast displays markers of senescence,<sup>44,45</sup> this could be a primary area of circRNA accumulation. Indeed, this is consistent with our in vitro findings of circRNA expression primarily in the syncytiotrophoblast.

Recently, circRNAs were identified as a potential forensic tool for estimating biological age in human blood,<sup>46</sup> which is an exciting leap from circRNA accumulation in animals to differential circRNA expression with age in humans. Other studies have shown differentially expressed circRNAs in human granulosa cells from women who were young vs those of advanced reproductive age<sup>47</sup> and that specific circRNAs in human peripheral blood were associated with parental longevity and cellular senescence.<sup>48</sup> The link between circRNA differential expression and Alzheimer's disease is becoming more widely investigated,<sup>49</sup> which is of particular interest to this study given

that Alzheimer's disease is, at its core, an aging disorder.<sup>50</sup> Although these studies demonstrate that the expression of circRNAs is *changed* among differently aged groups, none of these studies investigated circRNA *accumulation* in aging tissue.

We posit that the abundance of a circRNA is a combination of expression level and accumulation. circRNA expression level can be increased by overexpressing the linear gene or by alternative splicing that promotes the circular over the linear transcripts. circRNA accumulation indicates that the circRNA remains in the tissue,<sup>36</sup> unaffected by exoribonucleases.<sup>38</sup> Over time, the abundance of the circRNA in the tissue increases as the accumulated transcripts escape degradation. This occurs without a change in the linear gene expression or alternative splicing. The result is that these circRNAs can continually exert their function in the tissue well after their linear gene's expression and at a higher-than-expected abundance.

### Implications of circular RNA accumulation as a novel mechanism for placental aging

Like other tissues in the body, the placenta undergoes the normal phenomenon of aging. Tissue aging includes progressive increases in cellular senescence.<sup>51</sup> For the placenta, this implies a decline in functionality as gestational age increases, resulting in a reduced capacity of the placenta to support the fetus.<sup>3</sup> Placentae from stillbirths undergo an accelerated aging process,<sup>3</sup> exhibiting similar pathologic features regardless of their earlier gestational ages. Markers of aging, such as increased DNA and RNA oxidation, lipid peroxidation, altered perinuclear location of lysosomes, and larger autophagosomes, are found in placentae from stillbirths and those from healthy late-term pregnancies compared with placentae from healthy early-term pregnancies.<sup>3</sup> This study expands on the current literature, demonstrating that shorter telomeres, increased cellular senescence, and DNA breaks occur with placental aging.

A circR-loop is formed when a circRNA molecule binds to 1 strand of helicase-unwound genomic DNA.<sup>11</sup> The steric hindrance of this bulky structure causes RNA polymerase II to stall during transcription, resulting in a DNA break, and often a subsequent fusion at another locus,<sup>52</sup> promoting genomic instability.<sup>12</sup> Double-stranded DNA breaks are lethal to cells, because they affect both strands of DNA and promote the loss of genetic information.<sup>14</sup> Any type of DNA damage can trigger cellular apoptosis or senescence.<sup>13</sup> Given that we observed increased DNA breaks in stillbirth placentae, which also had an elevated abundance of circ\_0000284 binding to placental DNA, we further determined that circ\_0000284 induces DNA damage and cellular senescence in vitro. Moreover, RNase H1 was investigated as a proposed method of circRNA degradation. Knockdown of RNase H1 using siRNA revealed that a portion of all circRNAs are susceptible to RNase H1 degradation in placenta tissue; however, this was more impactful in placentae from unexplained stillbirth. This could be caused by a greater proportion of circRNAs susceptible to RNase H1 in tissue than circRNAs that are not susceptible, or could indicate a lack of endogenous RNase H1 in placentae from unexplained stillbirth. This would also potentially account for the premature circRNA accumulation in these samples. Together, this presents a promising avenue for investigation as a mechanism for stillbirth via premature placental aging. This study also provides evidence that circRNAs accumulate in healthy aging placental tissue and can also be detected as a novel proxy measure of placental aging in maternal blood.

### Clinical implications

Our group at 41+ weeks' gestation encompassed women who birthed between 41+1 and 41+6 weeks' gestation. Given that gestation of >40 weeks, in addition to a maternal age of  $\geq 35$  years<sup>3</sup> and male fetal sex,<sup>1</sup> is a risk factor for stillbirth, the current Pregnancy Care Guidelines consider 42 weeks' gestation

and beyond as post-term and recommend fetal monitoring and induction of labor from 41 weeks' gestation, even in uncomplicated, low-risk patients.<sup>53</sup> Indeed, evidence shows that stillbirth and neonatal death can be reduced with fetal surveillance twice weekly from 39 weeks.<sup>54</sup>

In this study, placentae from stillbirths displayed evidence of further aging hallmarks. Given that these stillbirth placentae were from stillbirths that occurred at gestational weeks 23, 26, 31, and 34, this clearly indicates that in stillbirth the placenta experiences accelerated tissue aging, resulting in a post-term phenotype much earlier than would be appropriate for their gestational age. The use of a blood test for signaling accelerated placental aging, as supported by our results, could be beneficial to screen for pregnancies at a high risk of stillbirth.

Senescence, as a product of tissue aging, is currently not assessed during autopsy. Routine histopathologic examination of the placenta typically involves macroscopic assessment (eg, size, weight, structure, cord insertion) and microscopic evaluation using hematoxylin and eosin staining. This allows for the identification of common pathologic features such as inflammation, infarction, or infection, which are also specifically ruled out during evaluation of unexplained stillbirths.<sup>55,56</sup> However, placental senescence is a molecular process that is not detectable by standard histology. The detection of senescence requires specialized assays, such as senescence-associated  $\beta$ -galactosidase staining, or molecular techniques such as immunofluorescence or qPCR targeting markers of DNA damage and cell cycle arrest (eg, p21,  $\gamma$ H2AX).<sup>57–59</sup> These are not part of routine clinical examination, and thus, a placenta affected by pathologic aging could appear entirely normal under conventional pathologic review.

### Research implications

Interpreting our results, we propose the following mechanism as a potential contributor to stillbirth pathology (Figure 5): in uncomplicated

pregnancies, circRNAs naturally accumulate in placental cells as the tissue ages with gestation. However, in pregnancies resulting in unexplained stillbirth, premature placental aging results in the accelerated accumulation of circRNAs. These circRNAs form circR-loops, with at least 1 circRNA (circ\_0000284) known to facilitate DNA damage and induce senescence. Given that DNA breaks facilitate genomic instability<sup>12</sup> and cellular senescence<sup>60</sup> and apoptosis,<sup>61</sup> this may result in reducing placental function to the detriment of the fetus.

### Strengths and limitations

We confirm that circRNAs accumulate in human aged tissue. Importantly, we established that there is no global increase in total RNA nor in circRNA abundance with placental gestational age; hence, our candidate circRNAs are unique in their ability to accumulate with age. It should be noted that the accumulation of these specific circRNAs with age may be placenta specific, given that this study only examined placental tissue, and this candidate list may not be exhaustive. Further studies will profile all accumulating circRNAs in the placenta as it ages.

It is worth noting that the fetal weights for the week 23 and week 31

stillbirths were pathologically low, whereas the others fell within the normal physiological range. These findings were not explained by fetal, placental, or genomic autopsy. However, no correlation was observed between fetal weight and the data presented in this study.

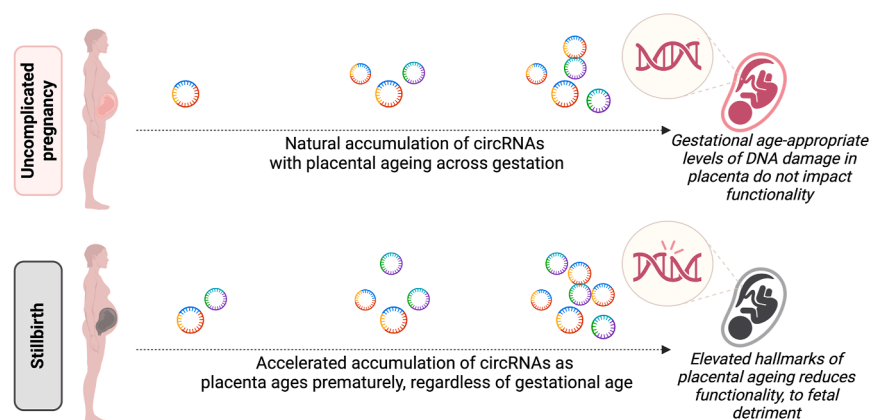
In addition, this study is limited by the small sample size of stillbirth placentae; however, this is a common issue in stillbirth research<sup>3,62</sup> given the difficulty in obtaining tissue within an appropriate time frame. Given that stillbirths that could be explained by fetal congenital abnormality were excluded, resulting in a pure “unexplained stillbirth” sample pool, this further reduced available tissue samples. Moreover, the sample size limited our ability to perform fetal sex-specific statistical tests. Further studies will be conducted with larger sample sizes to allow for increased comparisons. Future studies will also include participants of different ethnicities, accounting for ethnicities that are more prone to stillbirths (such as South Asian women<sup>54</sup>).

### Conclusions

circRNAs accumulate in aging human placental tissue, in the absence of any change in total linear or circRNA expression or alternative splicing

**FIGURE 5**

**Proposed mechanism by which circRNA accumulation and placental aging contribute to stillbirth**



circRNA, circular RNA.

Arthurs. Circular RNAs, placental aging, and stillbirth. *Am J Obstet Gynecol* 2026.

variants. Importantly, specific circRNAs are present at exceptionally high levels in placentae from stillbirths, similar to or surpassing the circRNA levels found in post-term placentae. We provide evidence that these circRNAs bind to DNA to form circR-loops in placental tissue. In vitro experiments in primary human syncytiotrophoblasts show that knockdown of circ\_000284 results in decreased DNA breaks in cells, indicating that this circRNA facilitates DNA damage, and decreased expression of senescence-associated genes, implying that this circRNA induces cellular senescence. Finally, measurement of candidate circRNAs in maternal blood sampled at 15 to 16 weeks' gestation has potential as a viable tool to screen for accelerated placental aging, as a proxy for the risk of stillbirth. ■

## Acknowledgments

We thank the women who consented to their placental tissue being used for this research. Thank you to the clinical and anatomic staff from the Women's and Children's Hospital and Lyell McEwin Hospital who were involved in the women's care and who collected and biopsied the placental samples. Thank you to Professor Jose Polo for his insightful suggestions. Figures were created using [BioRender.com](https://BioRender.com)

## References

1. Australian Institute of Health and Welfare. In: Australian Institute of Health and Welfare. 2018. Available at: <https://www.aihw.gov.au/reports-data/population-groups/mothers-babies/data>. Accessed April 9, 2024.
2. Hug L, You D, Blencowe H, et al. Global, regional, and national estimates and trends in stillbirths from 2000 to 2019: a systematic assessment. *Lancet* 2021;398:772–85.
3. Maiti K, Sultana Z, Aitken RJ, et al. Evidence that fetal death is associated with placental aging. *Am J Obstet Gynecol* 2017;217:441.e1–14.
4. Ferrari F, Facchinetti F, Saade G, Menon R. Placental telomere shortening in stillbirth: a sign of premature senescence? *J Matern Fetal Neonatal Med* 2016;29:1283–8. <https://doi.org/10.3109/14767058.2015.1046045>.
5. Amir H, Weintraub A, Aricha-Tamir B, Apel-Sarid L, Holcberg G, Sheiner E. A piece in the puzzle of intrauterine fetal death: pathological findings in placentas from term and preterm intrauterine fetal death pregnancies. *J Matern Fetal Neonatal Med* 2009;22:759–64.
6. Ebbesen KK, Hansen TB, Kjems J. Insights into circular RNA biology. *RNA Biol* 2017;14:1035–45.
7. Westholm JO, Miura P, Olson S, et al. Genome-wide analysis of drosophila circular RNAs reveals their structural and sequence properties and age-dependent neural accumulation. *Cell Rep* 2014;9:1966–80.
8. Cortés-López M, GRUNER MR, Cooper DA, et al. Global accumulation of circRNAs during aging in *Caenorhabditis elegans*. *BMC Genomics* 2018;19:8.
9. Gruner H, Cortés-López M, Cooper DA, Bauer M, Miura P. CircRNA accumulation in the aging mouse brain. *Sci Rep* 2016;6:38907.
10. Arthurs AL, Jankovic-Karasoulos T, Smith MD, Roberts CT. Circular RNAs in pregnancy and the placenta. *Int J Mol Sci* 2022;23:4551.
11. Conn SJ, Pillman KA, Toubia J, et al. The RNA binding protein quaking regulates formation of circRNAs. *Cell* 2015;160:1125–34.
12. Lord CJ, Ashworth A. The DNA damage response and cancer therapy. *Nature* 2012;481:287–94.
13. Parrinello S, Coppe JP, Krtolica A, Campisi J. Stromal-epithelial interactions in aging and cancer: senescent fibroblasts alter epithelial cell differentiation. *J Cell Sci* 2005;118:485–96.
14. Altaf M, Saksouk N, Côté J. Histone modifications in response to DNA damage. *Mutat Res* 2007;618:81–90.
15. Ren L, Jiang Q, Mo L, et al. Mechanisms of circular RNA degradation. *Commun Biol* 2022;5:1355.
16. Li X, Zhang JL, Lei YN, et al. Linking circular intronic RNA degradation and function in transcription by RNase H1. *Sci China Life Sci* 2021;64:1795–809.
17. Mohammed H, Roberts CT, Grzeskowiak LE, Giles LC, Dekker GA, Marshall HS. Safety and protective effects of maternal influenza vaccination on pregnancy and birth outcomes: a prospective cohort study. *EClinicalMedicine* 2020;26:100522.
18. Byrne AB, Arts P, Ha TT, et al. Genomic autopsy to identify underlying causes of pregnancy loss and perinatal death. *Nat Med* 2023;29:180–9.
19. Arthurs AL, Dietrich B, Knöfler M, et al. Genetically edited human placental organoids cast new light on the role of ACE2. *Cell Death Dis* 2025;16:78 (2025). <https://doi.org/10.1038/s41419-025-07400-x>.
20. Dietrich B, Kunihs V, Lackner AI, et al. Notch3 signalling controls human trophoblast stem cell expansion and differentiation. *Development* 2023;150:dev202152.
21. Haider S, Meinhardt G, Saleh L, et al. Self-renewing trophoblast organoids recapitulate the developmental program of the early human placenta. *Stem Cell Rep* 2018;11:537–51.
22. Tan JP, Liu X, Polo JM. Establishment of human induced trophoblast stem cells via reprogramming of fibroblasts. *Nat Protoc* 2022;17:2739–59.
23. Qi H, Xiong L, Tong C. Aging of the placenta. *Aging (Albany NY)* 2022;14:5294–5.
24. El Hage A, Webb S, Kerr A, Tollervey D. Genome-wide distribution of RNA-DNA hybrids identifies RNase H targets in tRNA genes, retrotransposons and mitochondria. *PLoS Genet* 2014;10:e1004716.
25. Alexander RD, Innocente SA, Barrass JD, Beggs JD. Splicing-dependent RNA polymerase pausing in yeast. *Mol Cell* 2010;40:582–93.
26. Wongsurawat T, Jenjaroenpun P, Kwok CK, Kuznetsov V. Quantitative model of R-loop forming structures reveals a novel level of RNA–DNA interactome complexity. *Nucleic Acids Res* 2012;40:e16.
27. Conn VM, Gabryelska M, Toubia J, et al. Circular RNAs drive oncogenic chromosomal translocations within the MLL recombinome in leukemia. *Cancer Cell* 2023;41:1309–26.e10.
28. Vilades D, Martínez-Cambor P, Ferrero-Gregori A, et al. Plasma circular RNA hsa\_circ\_0001445 and coronary artery disease: performance as a biomarker. *FASEB J* 2020;34:4403–14.
29. Drula R, Braicu C, Chira S, Berindan-Neagoe I. Investigating circular RNAs using qRT-PCR; roundup of optimization and processing steps. *Int J Mol Sci* 2023;24:5721.
30. Wu H, Lima WF, Zhang H, Fan A, Sun H, Crooke ST. Determination of the role of the human RNase H1 in the pharmacology of DNA-like antisense drugs. *J Biol Chem* 2004;279:17181–9.
31. Livak KJ, Schmittgen TD. Analysis of relative gene expression data using real-time quantitative PCR and the 2<sup>-ΔΔCT</sup> method. *Methods* 2001;25:402–8.
32. Cawthon RM. Telomere length measurement by a novel monochrome multiplex quantitative PCR method. *Nucleic Acids Res* 2009;37:e21.
33. Sanz LA, Chédin F. High-resolution, strand-specific R-loop mapping via S9.6-based DNA–RNA immunoprecipitation and high-throughput sequencing. *Nat Protoc* 2019;14:1734–55.
34. Morosin SK, Delforce SJ, Kahl RGS, Corbisier De Meaultsart C, Lumbers ER, Pringle KG. The (pro)renin receptor and soluble (pro)renin receptor in choriocarcinoma. *Reproduction* 2021;162:375–84.
35. Saul D, Kosinsky RL, Atkinson EJ, et al. A new gene set identifies senescent cells and predicts senescence-associated pathways across tissues. *Nat Commun* 2022;13:4827.
36. Knupp D, Miura P. CircRNA accumulation: a new hallmark of aging? *Mech Ageing Dev* 2018;173:71–9.
37. Hall H, MEDINA P, Cooper DA, et al. Transcriptome profiling of aging *Drosophila* photoreceptors reveals gene expression trends that correlate with visual senescence. *BMC Genomics* 2017;18:894.
38. Jeck WR, Sorrentino JA, Wang K, et al. Circular RNAs are abundant, conserved, and associated with ALU repeats. *RNA* 2013;19:141–57. <https://doi.org/10.1261/rna.035667.112>

39. Rybak-Wolf A, Stottmeister C, Glazar P, et al. Circular RNAs in the mammalian brain are highly abundant, conserved, and dynamically expressed. *Mol Cell* 2015;58:870–85.
40. Bachmayr-Heyda A, Reiner AT, Auer K, et al. Correlation of circular RNA abundance with proliferation—exemplified with colorectal and ovarian cancer, idiopathic lung fibrosis and normal human tissues. *Sci Rep* 2015;5:8057.
41. Song X, Zhang N, Han P, et al. Circular RNA profile in gliomas revealed by identification tool UROBORUS. *Nucleic Acids Res* 2016;44:e87.
42. Mayhew TM, Simpson RA. Quantitative evidence for the spatial dispersal of trophoblast nuclei in human placental villi during gestation. *Placenta* 1994;15:837–44.
43. Huppertz B, Frank HG, Reister F, Kingdom J, Korr H, Kaufmann P. Apoptosis cascade progresses during turnover of human trophoblast: analysis of villous cytotrophoblast and syncytial fragments in vitro. *Lab Invest* 1999;79:1687–702.
44. Chuprin A, Gal H, Biron-Shental T, et al. Cell fusion induced by ERVWE1 or measles virus causes cellular senescence. *Genes Dev* 2013;27:2356–66.
45. Goldman-Wohl D, Yagel S. United we stand not dividing: the syncytiotrophoblast and cell senescence. *Placenta* 2014;35:341–4.
46. Wang J, Wang C, Wei Y, et al. Circular RNA as a potential biomarker for forensic age prediction. *Front Genet* 2022;13:825443.
47. Cheng J, Huang J, Yuan S, et al. Circular RNA expression profiling of human granulosa cells during maternal aging reveals novel transcripts associated with assisted reproductive technology outcomes. *PLoS One* 2017;12:e0177888.
48. Haque S, Ames RM, Moore K, et al. circRNAs expressed in human peripheral blood are associated with human aging phenotypes, cellular senescence and mouse lifespan. *Geroscience* 2020;42:183–99. <https://doi.org/10.1007/s11357-019-00120-z>.
49. Akhter R. Circular RNA and Alzheimer's disease. *Adv Exp Med Biol* 2018;1087:239–43.
50. Smith MA, Sayre LM, Monnier VM, Perry G. Radical AGEing in Alzheimer's disease. *Trends Neurosci* 1995;18:172–6.
51. Holt DJ, Grainger DW. Senescence and quiescence induced compromised function in cultured macrophages. *Biomaterials* 2012;33:7497–507.
52. Conn VM, Hugouvieux V, Nayak A, et al. A circRNA from SEPALLATA3 regulates splicing of its cognate mRNA through R-loop formation. *Nat Plants* 2017;3:17053.
53. Australian\_Government\_Department\_of\_Health Department of Health, ed. Canberra; 2020. Available at: [https://files.magicapp.org/guideline/3aa6b881-4be5-4806-bb3e-e7c53b5b0bbf/published\\_guideline\\_7933-2\\_0.pdf](https://files.magicapp.org/guideline/3aa6b881-4be5-4806-bb3e-e7c53b5b0bbf/published_guideline_7933-2_0.pdf). Accessed May 12, 2024.
54. Davies-Tuck ML, Davey MA, Hodges RL, Wallace EM. Fetal surveillance from 39 weeks' gestation to reduce stillbirth in South Asian-born women. *Am J Obstet Gynecol* 2023;229:286.e1–9.
55. Khong TY, Mooney EE, Ariel I, et al. Sampling and definitions of placental lesions: Amsterdam placental workshop group consensus statement. *Arch Pathol Lab Med* 2016;140:698–713.
56. Redline RW, Roberts DJ, Parast MM, et al. Placental pathology is necessary to understand common pregnancy complications and achieve an improved taxonomy of obstetrical disease. *Am J Obstet Gynecol* 2023;228:187–202.
57. Sharpless NE, Sherr CJ. Forging a signature of in vivo senescence. *Nat Rev Cancer* 2015;15:397–408.
58. Coppé J-P, Desprez P-Y, Krtolica A, Campisi J. The senescence-associated secretory phenotype: the dark side of tumor suppression. *Annu Rev Pathol* 2010;5:99–118.
59. Velarde MC, Demaria M. Targeting senescent cells: possible implications for delaying skin aging: a mini-review. *Gerontology* 2016;62:513–8.
60. McHugh D, Gil J. Senescence and aging: causes, consequences, and therapeutic avenues. *J Cell Biol* 2018;217:65–77.
61. Baar MP, Brandt RMC, Putavet DA, et al. Targeted apoptosis of senescent cells restores tissue homeostasis in response to chemotoxicity and aging. *Cell* 2017;169:132–47.e16.
62. Hannan NJ, Stock O, Spencer R, et al. Circulating mRNAs are differentially expressed in pregnancies with severe placental insufficiency and at high risk of stillbirth. *BMC Med* 2020;18:145. <https://doi.org/10.1186/s12916-020-01605-x>.

## Author and article information

From the Flinders Health and Medical Research Institute, Flinders University, Adelaide, South Australia, Australia (Arthurs, McCullough, Webb, Smith, Jankovic-Karasoulos, and Roberts); College of Medicine and Public Health, Flinders University, Adelaide, South Australia, Australia (Arthurs, McCullough, Webb, Smith, Jankovic-Karasoulos, and Roberts); School of Biomedicine and Robinson Research Institute, The University of Adelaide, Adelaide, South Australia, Australia (Arthurs); Department of Genetics and Molecular Pathology, SA Pathology, Adelaide, South Australia, Australia (Jackson, Scott, and Webb); Centre for Cancer Biology, an alliance between SA Pathology and the University of South Australia, Adelaide, South Australia, Australia (Jackson and Scott); Australian Genomics, Parkville, Victoria, Australia (Jackson); Adelaide Medical School, The University of Adelaide, Adelaide, South Australia, Australia (Scott and Barnett); ACRF Genomics Facility, Centre for Cancer Biology, an alliance between SA Pathology and the University of South Australia, Adelaide, South Australia, Australia (Scott); UniSA Clinical and Health Sciences, University of South Australia, Adelaide, South Australia, Australia (Scott); Paediatric and Reproductive Genetics Unit, South Australian Clinical Genetics Service, Women's and Children's Hospital, North Adelaide, South Australia, Australia (Barnett); and Department of Obstetrics and Gynecology, Lyell McEwin Hospital, The University of Adelaide, Adelaide, South Australia, Australia (Dekker).

Received April 6, 2025; revised Aug. 7, 2025; accepted Aug. 21, 2025.

Provisional patent (ALA and CTR) # 2024902762 was filed on September 2, 2024. The remaining authors report no conflict of interest.

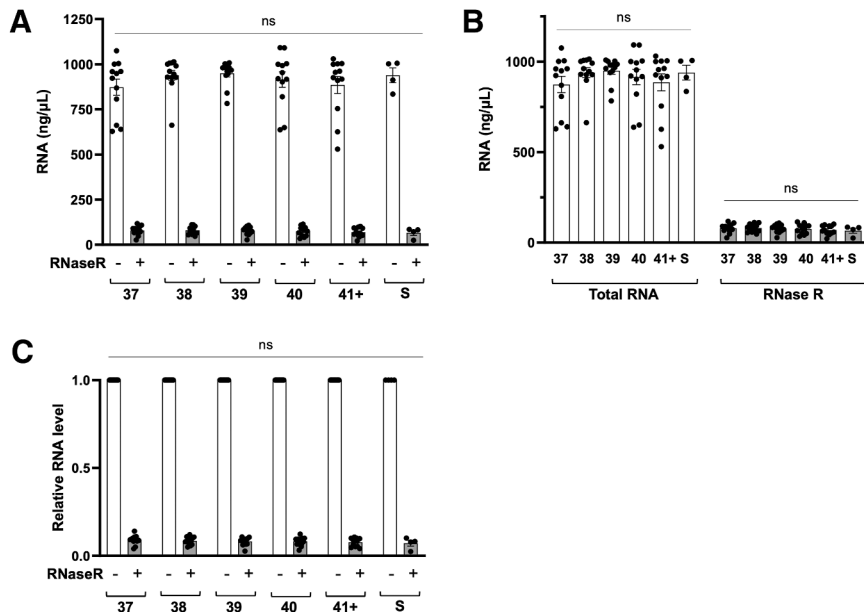
ALA is supported by funding from the Flinders Foundation, Flinders University, the Channel 7 Children's Research Foundation, and a Future Making Fellowship from The University of Adelaide. CTR is supported by a National Health and Medical Research Council (NHMRC) Investigator Grant (GNT1174971) and a Matthew Flinders Fellowship from Flinders University.

The Genomic Autopsy Study was supported by NHMRC (#APP1123341), Genomics Health Futures Mission — Medical Research Future Fund (#GHFM76777), and the Australian Genomic Health Alliance NHMRC Targeted Call for Research into Preparing Australia for the Genomics Revolution in Healthcare (#GNT1113531) to HSS and CPB.

Corresponding author: Anya L. Arthurs, PhD. [anya.arthurs@flinders.edu.au](mailto:anya.arthurs@flinders.edu.au)

## SUPPLEMENTAL FIGURE 1

## Concentration and quantity of RNA per sample group

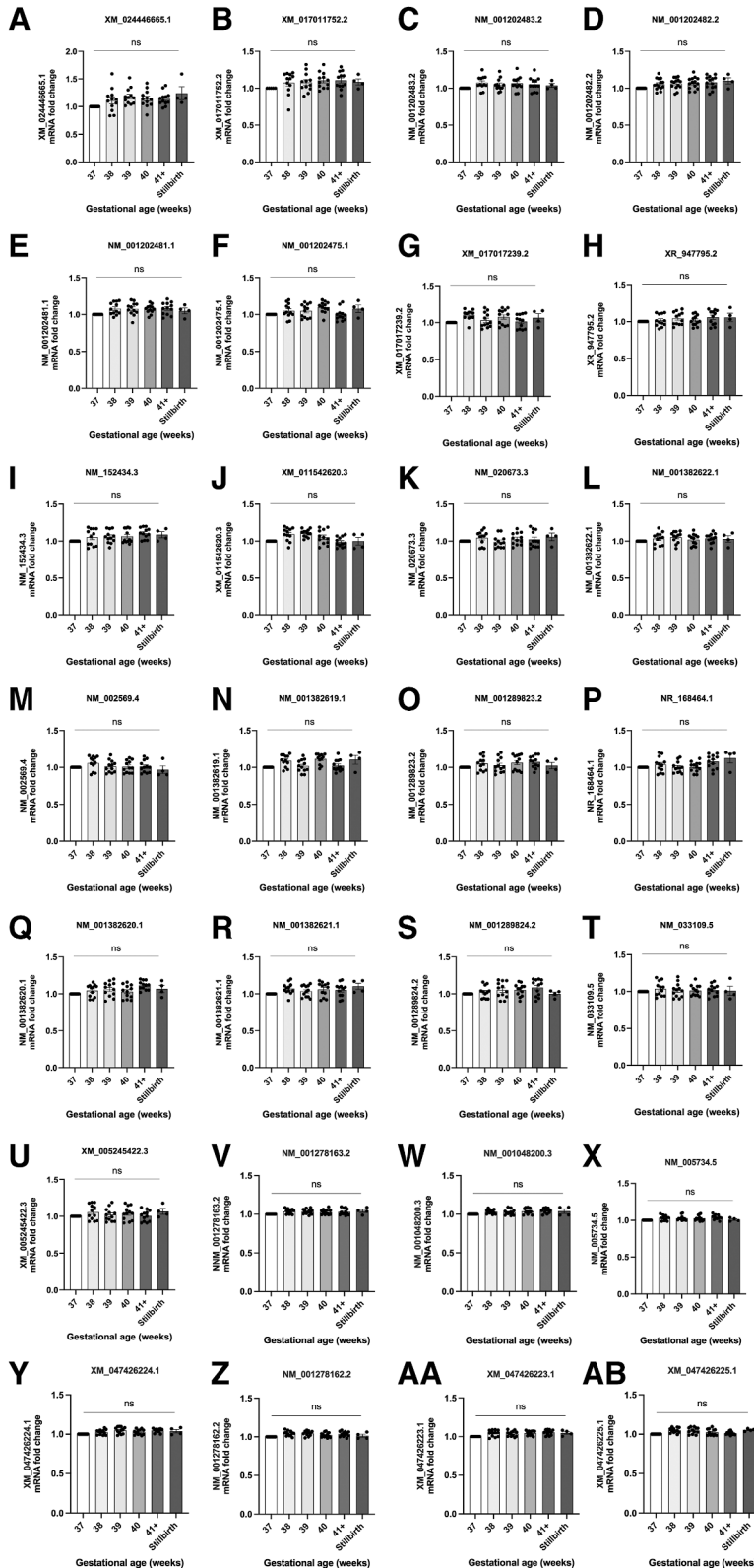


**A, B**, RNA concentration ( $\text{ng}/\mu\text{L}$ ) and **(C)** abundance (as fold change of RNase R–depleted RNA relative to total RNA) in isolated cells from 37, 38, 39, 40, and 41+ uncomplicated and stillbirth (S) placentae.  $n=12$  placentae/uncomplicated gestational group,  $n=4$  stillbirth placentae. RNA was extracted from each sample, then split into 2 aliquots; the first was untreated (total RNA), whereas the second was digested with RNase R (leaving only circRNAs). RNA concentration and abundance of total RNA and RNase R–digested RNA were assessed to determine whether these changed across gestation or in stillbirth. Data are presented as scatter plots with bars and indicate mean  $\pm$  standard error of the mean.

circRNA, circular RNA; ns, not significant.

Arthurs. Circular RNAs, placental aging, and stillbirth. *Am J Obstet Gynecol* 2026.

**SUPPLEMENTAL FIGURE 2**  
**Cognate gene expression for candidate circRNAs**



←  
 NM\_001202482.2, (E) NM\_001202481.1, and (F) NM\_001202475.1; linear CWF19L2 gene variants (G) XM\_017017239.2, (H) XR\_947795.2, (I) NM\_152434.3, and (J) XM\_011542620.3; linear RAB22A gene variant (K) NM\_033109.5; linear FURIN gene variants (L) NM\_001382622.1, (M) NM\_002569.4, (N) NM\_001382619.1, (O) NM\_001289823.2, (P) NR\_168464.1, (Q) NM\_001382620.1, (R) NM\_001382621.1, and (S) NM\_001289824.2; linear PNPT1 gene variant (T) NM\_033109.5; linear PAPP2 gene variant (U) XM\_005245422.3; and linear HIPK3 gene variants (V) NM\_001278163.2, (W) NM\_001048200.3, (X) NM\_005734.5, (Y) XM\_04746224.1, (Z) NM\_001278162.2, (AA) XM\_047426223.1, and (AB) XM\_047426225.1 all in isolated cells from 37, 38, 39, 40, and 41+ uncomplicated and stillbirth placentae. n=12 placentae/uncomplicated gestational group, n=4 stillbirth placentae. Data are presented as scatter plots with bars and indicate mean±standard error of the mean.

ns, not significant.

Arthurs. Circular RNAs, placental aging, and stillbirth. *Am J Obstet Gynecol* 2026.

Abundance (as fold change relative to abundance at 37 weeks' gestation) of linear CRHR2 gene variants (A) XM\_024446665.1, (B) XM\_017011752.2, (C) NM\_001202483.2, (D)

## SUPPLEMENTAL TABLE 1

## Materials required for the preparation of TSC, syncytiotrophoblast, and extravillous trophoblast differentiation media

Component	Concentration	Manufacturer
TSC media		
DMEM/F12 GlutaMAX	Base media	Gibco
B-27	1×	Gibco
Insulin-Transferrin-Selenium-Ethanolamine (ITS-X)	1×	Gibco
A83-01	1 μM	Tocris
Recombinant human epidermal growth factor (rhEGF)	50 ng/mL	R&D Systems
CHIR99021	2 μM	Tocris
Y27632	5 μM	Santa Cruz
Syncytiotrophoblast differentiation media		
DMEM/F12 GlutaMAX	Base media	Gibco
Bovine serum albumin (BSA)	0.3% (wt/vol)	Sigma-Aldrich
Insulin-Transferrin-Selenium-Ethanolamine (ITS-X)	1×	Gibco
A83-01	7.5 μM	Tocris
2-mercaptoethanol	0.1 mM	Sigma-Aldrich
Y27632	2.5 μM	Santa Cruz
KnockOut serum replacement (KSR)	4% (vol/vol)	Thermo Fisher Scientific
Forskolin	2 μM	Sigma-Aldrich
Extravillous trophoblast differentiation media		
DMEM/F12 GlutaMAX	Base media	Gibco
Bovine serum albumin (BSA)	0.3% (wt/vol)	Sigma-Aldrich
Insulin-Transferrin-Selenium-Ethanolamine (ITS-X)	1×	Gibco
A83-01	7.5 μM	Tocris
2-mercaptoethanol	0.1 mM	Sigma-Aldrich
Y27632	2.5 μM	Santa Cruz
KnockOut serum replacement (KSR)	4% (vol/vol)	Thermo Fisher Scientific
hNRG1-β1 <sup>a</sup>	100 ng/mL	Cell Signaling Technology

TSC, trophoblast stem cell.

<sup>a</sup> NB! Add to the media only for the first 6 d of culture, then remove.

Arthurs. Circular RNAs, placental aging, and stillbirth. *Am J Obstet Gynecol* 2026.

**SUPPLEMENTAL TABLE 2**  
**Primer sequences and T<sub>m</sub> used for qPCR**

Gene	Transcript	Forward primer	Reverse primer	T <sub>m</sub>
<i>CRHR2</i>	XM_024446665.1	ATGGACGCGGCACTGCT	ACTGCAGCCTGGCGCT	57
	XM_017011752.2	TCCTACTGCAACACGACCTT	GTTGATCTTTGAGGCCACG	59
	NM_001202483.2	AGAAAGAGATGTGTGCCAAGC	CCAGAGGAAGAAGGTGGAGG	58
	NM_001202482.2	CTCACTCTCGCGTCCACTC	GTTGATCTTTGAGGCCACG	59
	NM_001202481.1	GGTCAAATGGGAAGAGAGCC	GTGTTGACTTGACGCCGTT	58
	NM_001202475.1	CATGACCCTCACCAACCTCT	AAGGTCGTGTGCAGTAGGA	58
	Circular: circ_0009000	TGGCTACAATTCTGCTCCA	ACATCTGCTGCTTTGTGTGG	59
<i>CWF19L2</i>	XM_017017239.2	AGATGGTGGATTAAGCTGGCT	GAATGGACTCACGCTCTGGA	59
	XR_947795.2	CCAGAAAGGGAGTATGAACAAAC	CCATGTCACCCACTTCCTTG	57
	NM_152434.3	AGCCATCGGAAACCACTACT	CCATGTCACCCACTTCCTTG	58
	XM_011542620.3	TCATGGAGTCGCTCTGATGG	ACATCAGGGAATGGGCTCTT	58
	Circular: circ_0024157	AGAAGTGATATACCATTCTTAAATGTA	GATAAATTACAAAATTACATGGATAA	53
<i>RAB22A</i>	NM_020673.3	TATTGTGTGGCGGTTTGTGG	TCTTGCCAGCTGTATCCCA	58
	Circular: circ_0061017	CCCATTGGCTGAACTCTTCC	AGCCACTACACTTGTCTTGA	57
<i>FURIN</i>	NM_001382622.1	GCATCATCGACATCCTCACC	GTCTCCACGTCATTCTCGGT	58
	NM_002569.4	ACATCCTCACCGAGCCCA	GACTCTCGGCTGCTCTGG	59
	NM_001382619.1	GTGCAGTCTCCCTCGAC	TCACTCCTCGATGCCAGAAG	59
	NM_001289823.2	CGGTCGCCTGGAAAAGTT (distinguished by product size)	CTGGACGATGGCATCGAGA	58
	NR_168464.1			
	NM_001382620.1	GACTCGGGTGCGGGATC	TGTTGCTGCTACCACCATA	58
	NM_001382621.1	CCAAGAACACAGCCAGGAAG	TACCACCATAGCAACCAGG	58
	NM_001289824.2	GGTTTGAGACAACTGGGACTAG	GACCAAGGTTCTGTTGCTG	58
Circular: circ_0036877	TTTGTAAGATGCTGGGTTGGTG	ACTGCATCTGTCACCTCGC	57	
<i>PNPT1</i>	NM_033109.5	CCTCCCAGTTTATGCCCTTGG	AAAGAGCGGCTAATTGAACGAT	60
	Circular: circ_0054624	AGCATGTTAGGCAATGTTGAT	TTTACTGACCGCTGTGACCA	60
<i>PAPPA2</i>	XM_005245422.3	GCATCTCAGCTGTGGCTCTA	AGTTACTGGGAGCCGAAAGAC	56
	Circular: circ_0111277	AGTCGATGGATTCCTCTCAT	AAGTTGTTCACTACTCTGTT	55
<i>HIPK3</i>	NM_001278163.2	GTCTTTGGGAGTTAAACCGACT	ACACAAGTCTTTGGCTCTAC	59
	NM_001048200.3	GTTTCGCCGTTTCTCTCAG (distinguished by product size)	ACTTCTCGACATCTTTCCCA	60
	NM_005734.5			
	XM_047426224.1	GCAGTCTAGGCCGTAATA (distinguished by product size)	ACTTCTCGACATCTTTCCCA	60
	XM_047426223.1			
	XM_047426225.1	ATGGAGCAGAGTCTTTGA	TTGCCGCTGTTGTCTGAAA	59
	NM_001278162.2	AGGGAGACGGCTGTTGTAAG	ACACAAGTCTTTGGCTCTAC	60
Circular: circ_0000284	CTGTGATTTTCAGCTGGCCT	GATGGGTGGCAAATCAAATGT	58	
<i>YWHAZ</i>		ACCGTTACTTGGCTGAGGTTGC	CCCAGTCTGATAGGATGTGTTGG	60
<i>GAPDH</i>		TCAAGGCTGAGAACGGGAAG	CGCCCCACTTGATTTGGAG	60
<i>ACT1B</i>		CACCATTGGCAATGAGCGGTTG	AGGTCTTTGCGGATGTCCACGT	60
<i>CXCL8</i>		AAGCTGGCCGTGGCTCTCTTG	AGCCCTCTTCAAAAATTCTC	60

Arthurs. Circular RNAs, placental aging, and stillbirth. *Am J Obstet Gynecol* 2026.

(continued)

## SUPPLEMENTAL TABLE 2

Primer sequences and  $T_m$  used for qPCR (continued)

Gene	Transcript	Forward primer	Reverse primer	$T_m$
<i>CST3</i>		CAACAAAGCCAGCAACGACA	TCTTGGTACACGTGGTTCGG	60
<i>TYROBP</i>		ACTGAGACCGAGTCGCCTTAT	ATACGGCCTCTGTGTGTTGAG	61
<i>FCER1G</i>		AGCAGTGGTCTTGCTTACT	TGCCTTCGCACCTGGATCTT	62
<i>LYZ</i>		CTTGTCCTCCTTTCTGTTACGG	CCCCTGTAGCCATCCATTCC	60
<i>CCL3</i>		TTCTCTGTACCATGACACTCTGC	CGTGGAAATCTCCGGCTGTAG	61
<i>CTSS</i>		CCATTGGGATCTCTGGAAGAAAA	TCATGCCCACTTGGTAGGTAT	59
<i>AIF1</i>		ATCAACAAGCAATTCCTCGATGA	CAGCATTGCTTCAAGGACATA	60
<i>HMGA1</i>		GCTGGTAGGGAGTCAGAAGGA	TGGTGGTTTTCCGGGTCTTG	62
<i>HIRA</i>		TTCAGTTGATATTCACCCTGACG	AAGTGATTGTCCATCTGGCAAA	59

$T_m$ , melt temperature; qPCR, quantitative polymerase chain reaction.

Arthurs. Circular RNAs, placental aging, and stillbirth. *Am J Obstet Gynecol* 2026.

## SUPPLEMENTAL TABLE 3

**P values for circRNA abundance comparisons between gestational age groups and the stillbirth group**

		Gestational age group (wk)			
		39	40	41+	Stillbirth
<b>circ_0009000</b>					
Wk	37		$P=.0005$	$P<.0001$	$P<.0001$
	38		$P=.0079$	$P<.0001$	$P=.0006$
	39				
		Gestational age group (wk)			
		39	40	41+	Stillbirth
<b>circ_0024157</b>					
Wk	37		$P=.0003$	$P<.0001$	$P<.0001$
	38			$P=.0002$	$P=.0027$
	39			$P=.0124$	$P=.0336$
		Gestational age group (wk)			
		39	40	41+	Stillbirth
<b>circ_0061017</b>					
Wk	37	$P=.0260$	$P<.0001$	$P<.0001$	$P<.0001$
	38		$P=.0053$	$P=.0003$	$P=.0034$
	39				
		Gestational age group (wk)			
		39	40	41+	Stillbirth
<b>circ_0036877</b>					
Wk	37	$P=.0151$	$P=.0002$	$P<.0001$	$P<.0001$
	38			$P<.0001$	$P=.0038$
	39				
		Gestational age group (wk)			
		39	40	41+	Stillbirth
<b>circ_0054624</b>					
Wk	37		$P<.0001$	$P<.0001$	$P<.0001$
	38		$P=.0232$	$P<.0001$	$P=.0012$
	39			$P=.0138$	
		Gestational age group (wk)			
		39	40	41+	Stillbirth
<b>circ_0111277</b>					
Wk	37	$P=.0443$	$P=.0002$	$P<.0001$	$P<.0001$
	38			$P=.0003$	$P=.0142$
	39			$P=.0050$	
		Gestational age group (wk)			
		39	40	41+	Stillbirth
<b>circ_0000284</b>					
Wk	37		$P<.0001$	$P<.0001$	$P<.0001$
	38			$P<.0001$	$P=.0042$
	39			$P=.0158$	

circRNA, circular RNA.

Arthurs. Circular RNAs, placental aging, and stillbirth. Am J Obstet Gynecol 2026.